Quantitative model of Carbon and Nitrogen isotope composition to highlight sources of nutrient discharge in coastal area (Toulon Bay, NW Mediterranean Sea)

Duc Huy Dang, R. Douglas Evans, Gaël Durrieu, Amonda El Houssainy, Jean-Ulrich Mullot, N. Layglon, Véronique Lenoble, Stéphane Mounier, Cédric Garnier

▶ **To cite this version:**

HAL Id: hal-01879413
https://hal.science/hal-01879413

Submitted on 29 Sep 2018

1   **Quantitative model of Carbon and Nitrogen isotope composition to highlight sources of**

2   **nutrient discharge in coastal sediments (Toulon Bay, NW Mediterranean Sea)**

3

4   Duc Huy Dang[1,2*], R. Douglas Evans[1,3], Gael Durrieu[2,4], Nicolas Layglon[2], Amonda El

5   Houssainy[2,5], Jean-Ulrich Mullot[6], Véronique Lenoble[2,4], Stéphane Mounier[2,4], Cédric

6   Garnier[2,4]

7

8   [1] School of the Environment, Trent University, 1600 West Bank Drive, Peterborough, ON,

9   Canada K9L 0G2

10   [2] Université de Toulon, PROTEE, EA 3819, CS60584, 83041 Toulon Cedex 9, France

11   [3] Water Quality Centre, Trent University, 1600 West Bank Drive, Peterborough, ON, Canada

12   K9L 0G2

13   [4] Université de Toulon, Aix Marseille Université, CNRS, IRD, Mediterranean Institute of

14   Oceanography (MIO), UMR7294, 83041 Toulon Cedex 9, France

15   [5] Centre National des Sciences Marines, CNRSL, PO Box 534, Batroun, Lebanon

16   [6] LASEM-Toulon, Base Navale De Toulon, BP 61, 83800 Toulon, France

17

18   *Corresponding author. Tel: +1 705 748 1011 (ext. 7692).

19   *E-mail:* huydang@trentu.ca

20

ABSTRACT

Nutrient loadings from either point or non-point sources to the environments are related to the growing global population. Subsequent negative impacts of nutrient loading on the environments requires a better understanding of their biogeochemical cycling and better tools to track their sources. This study examines the C, N and P discharge and cycling in a Mediterranean coastal area from rivers to marine sediments and assesses the anthropogenic contributions. Carbon and N concentrations and isotope compositions in rivers particles, surface sediments, and sediment cores were investigated to build up a quantitative multiple-end-member mixing model for C and N isotopes. This model has allowed determining the contribution of four natural and one anthropogenic sources to the sediments and highlighted the anthropogenic fraction of P based on the relationship with anthropogenic $\delta^{15}N$. Although P is a monoisotopic element and P total concentration has been the sole index to study P loading, this study suggests an alternative approach to differentiate anthropogenic and non-anthropogenic (diagenetic) P and revealed point and non-point sources of P and the corresponding P loading. Also, the diagenetic P background has been established for the 50-cm sediment layer of the whole Bay.

1. INTRODUCTION

Coastal and estuarine areas are among the most productive, diverse, and economically important ecosystems for human society, and play a primordial role in C and other nutrients storage via primary production. However, these ecosystems are widely and globally threatened, mostly by anthropogenic pressure and impacts of climate change (Hobbie, 2000; Paerl, 2006; UNEP, 2006; Wetz et al., 2008). One of the greatest threats to these ecosystems is eutrophication due to nutrients loading by either point (e.g. waste water discharge) or non-point (e.g. agricultural runoff, atmospheric deposition) sources (Bohlin et al., 2006; Church et al., 2006; Savage et al., 2010; Vaalgamaa et al., 2013) leading to an increasing frequency of harmful algal blooms (Kimbrough et al., 2008; Paerl, 2008, 2006; Vitousek et al., 1997).

Sedimentary accumulation in organic matter (OM) and C-N isotope composition have been used widely as a valuable paleo-environmental tool to track origins of the OM and any change in nutrient availability in surface waters (Bohlin et al., 2006; Church et al., 2006; Di Leonardo et al., 2012; Harmelin-Vivien et al., 2008; Ogrinc et al., 2005; Teranes and Bernasconi, 2000; Vaalgamaa et al., 2013; Yokoyama et al., 2006). The carbon source for terrestrial plants is atmospheric CO_2 with a $\delta^{13}C$ which decreased from -7.5‰ in the 1980s to -8.5‰ today, relative to the Vienna PeeDee Belemnite (Cuntz, 2011). For land vegetation, different assimilation pathways differentiate C3 and C4 plants by typical $\delta^{13}C$ ranges of -24‰ to -34‰ and -10‰ to -20‰, respectively (Dean, 2006; Meyers, 1997). However, most aquatic vegetation obtains its carbon from dissolved inorganic carbon resulting in $\delta^{13}C$ ranging from -18 to -28 ‰ (Bohlin et al., 2006; Dean, 2006; Kendall et al., 2001). The two latter OM pools of terrestrial plants (i.e., land and aquatic) are then indistinguishable by $\delta^{13}C$. However, there is a significant difference in $\delta^{13}C$ between terrestrial and marine organic matter (freshwater and marine phytoplankton: -30 ‰ and 20-22‰, respectively (Bohlin et al., 2006; Bouillon et al., 2012; Meyers, 1997)). Also, among aquatic marine macrophytes, physiological

66 differences result in variation in $\delta^{13}C$ values in seagrasses and macroalgae (Parker, 1964;

67 Stephenson et al., 1986); a value of -10.5±3.3 ‰ has been reported in 195 observations of

68 seagrasses (Hemminga and Mateo, 1996) while a range from -12 to -18 ‰ is observed for

69 macroalgae (Belicka et al., 2012).

70 Concerning N, biogeochemical processes tend to enrich ^{15}N leading to a positive drift in $\delta^{15}N$,

71 except for some methanogenic and nitrogen-fixing organisms (e.g., cyanobacteria) (Cloern et

72 al., 2002; Dean, 2006). Relative to atmospheric N_2, $\delta^{15}N$ ranges from +2‰ to +3‰ in soils

73 (Vaalgamaa et al., 2013), and -2‰ to +5‰ in chemical fertilizers (Vaalgamaa et al., 2013)

74 while it ranges between +7‰ to +9‰ in estuarine and marine phytoplankton (Cloern et al.,

75 2002; Vaalgamaa et al., 2013). Also, a peculiarly high value of $\delta^{15}N$ between 10‰ to 25 ‰ is

76 typical of ammonia volatilization in animal manure (Choi et al., 2003) and could be used to

77 track agricultural and urban point sources (e.g., treated/untreated sewage discharge) (Bohlin et

78 al., 2006; Savage et al., 2010; Vaalgamaa et al., 2013). In summary, terrigenous material has

79 lower values in $\delta^{15}N$ and $\delta^{13}C$ than estuarine and marine OM (Ogrinc et al., 2005; Vaalgamaa

80 et al., 2013).

81 Diverse C-N isotope compositions reflect different sources of the OM. Also, early diagenesis

82 could alter the C-N isotope composition in sediments, mostly by selective degradation of

83 organic compounds and isotope fractionation during degradation (Ogrinc et al., 2005 and

84 references therein). However, this alteration is considered less significant for C (i.e., <2‰)

85 than N (Bohlin et al., 2006; Ogrinc et al., 2005). Nevertheless, contradictory conclusions have

86 been reported for the direction of N isotopic shift during decomposition. It finally appears that

87 the observed change in N isotopic composition (if any) is not related to that in the residual N

88 pool but to the microbially added nitrogen which depends on the N substrate (see discussion

89 in Bouillon et al. (2012) and Lehmann et al. (2002)). This conclusion supports the hypothesis

90 that the vertical variation in C and N isotope composition in sediments could be a useful tool

91   to track changes in organic matter input (Church et al., 2006; Teranes and Bernasconi, 2000)

92   when diagenetic alterations could be negligible (Engel and Macko, 2013; Kohzu et al., 2011).

93   In addition, eutrophication history could be recorded by C-N isotopes; previous studies

94   (Church et al., 2006; Teranes and Bernasconi, 2000) have reported (i) a significant positive

95   correlation between δ^{13}C and total sediment P indicating variations in primary production and

96   (ii) a change in sedimentary δ^{15}N related to an increase in dissolved nitrate, either by algal

97   uptake or a variation in N sources (e.g., wastewater vs. agricultural inputs). However, the

98   diagenetic P cycling is complex; P deposits in sediments in either inorganic or organic forms

99   which are both releasable in porewater due to carrier phase dissolution (e.g., iron

100   oxyhydroxides) and organic matter decomposition, potentially followed by P scavenging via

101   adsorption and/or precipitation processes (Anschutz et al., 2007; Dang et al., 2014a; Krom

102   and Berner, 1981; Ruttenberg, 2003). Therefore, it is not evident to decipher diagenetic P

103   enrichment from anthropogenic P in sediments (Anschutz et al., 2007; Dang et al., 2014b;

104   Ruttenberg, 2003). Unlike C and N, P is a monoisotopic element; it is not possible to track the

105   P sources and biogeochemical processes controlling P cycling by isotope composition.

106   Globally speaking, the nutrient cycling in coastal areas is challenging due to (i) a multiplicity

107   of sources (several natural and anthropogenic components), (ii) complex biogeochemical

108   processes capable of altering original isotope compositions and (iii) reciprocal interactions

109   with primary production. Resolving this complex system would permit a better evaluation of

110   the contribution from each source and pinpoint human signatures on nutrient inputs to the

111   vulnerable coastal areas. However, although multiples OM sources have been identified in

112   natural coastal sediments, simple mixing models have been used widely with only two end-

113   members as terrestrial and marine materials (Bohlin et al., 2006; Harmelin-Vivien et al., 2008;

114   Li et al., 2016; Loneragan et al., 1997; Ogrinc et al., 2005; Ramaswamy et al., 2008). Scarce

115   are studies on natural sediments with the application of a quantitative multiple-end-member

116   mixing model (Das et al., 2008). However, stable isotope mixing models using multiple

117   sources have been widely used in food-web studies (see discussion in Erhardt et al. (2014)

118   and Phillips et al. (2014)). This study aims at developing a quantitative multiple-end-member

119   mixing model for C and N isotope composition in the coastal sediments of Toulon Bay (NW

120   Mediterranean Sea) to better highlight anthropogenic contributions to the nutrient balance

121   (either by point or non-point sources) and sedimentary cycling of these nutrients. The

122   proposed model is based on C, N, P, Mg and I concentrations and C, N isotope compositions

123   in several samples of river particles, surface sediments and 50-cm sediment cores at eight

124   stations of the Bay.

125

126   **2. MATERIALS AND METHODS**

127   **2.1. Study site and sampling**

128   Samples were collected in Toulon Bay (Fig. 1, NW Mediterranean, SE French coast), hosting

129   the French Navy Base, yacht clubs, marinas, and aquaculture. Two small urbanized rivers

130   (Las and Eygoutier) and two treated sewage submarine outlets are the main

131   terrestrial/anthropogenic inputs to the sea (point sources), in addition to land runoff (non-point

132   source). The Bay is divided into two non-equal parts, an enclosed western little Bay and a

133   large Bay open to the sea. Previous studies have revealed serious contamination of the entire

134   ecosystem of Toulon Bay, and the situation is more dramatic in little Bay than large Bay

135   (Cossa et al., 2014; Dang et al., 2015a, 2015b, 2014b; Pougnet et al., 2014; Tessier et al.,

136   2011); in little Bay, the seagrass meadow of *Posidonia oceanica* have totally disappeared for

137   the last 30 years, harmful phytoplankton has proliferated, and zooplankton diversity was poor

138   (Bernard et al., 2001; Jamet et al., 2005; Jean et al., 2012).

139   With the support of the French Navy (boats, materials, divers), undisturbed surface and

140   subsurface sediments (0-5 and 5-10 cm, respectively) were collected from 54 stations situated

141 around the whole Toulon Bay (Fig. 1) using a sediment corer (10-cm diameter and 1-m long

142 Plexiglas tube) that preserved the sediment-water interface (SWI) (Tessier et al., 2011) in

143 December 2008, February and June 2009. In addition, sediment cores (~50 cm long) were

144 collected at eight specific stations (MIS, 3B, LAS1, LAS2, 12, 15, 23 and 52, Fig. 1) during

145 several sampling campaigns from June 2009 to May 2016 (Dang et al., 2015a). Stations

146 LAS1, LAS2 and 23 are situated in front of the two main active tributaries of the Bay (Las

147 and Eygoutier Rivers, Fig. 1) while the former Las river discharged close to station MIS

148 before it was diverted. Stations MIS, 3B and 12 are located in active military zones with

149 intense ship traffic, and station 15 is situated in an aquaculture area (fish and mussel farming).

150 Station 52 is located in large Bay. Sediments were sliced every 2 cm and centrifuged (4000

151 rpm, 15 min, Sigma 3-18K) within 2 h of collection under inert atmosphere (N_2). Pore waters

152 were extracted by filtration of collected supernatants (0.2- m in-line syringe filters, cellulose

153 nitrate, Sartorius) in an N_2-purged glove box.

154 In the two tributaries (Las and Eygoutier Rivers), particles traps were deployed by the IRSN

155 (Radioprotection and Nuclear Safety Institute). Five particle samples were collected in each

156 tributary during a two-week period from October 2012 to May 2013, mostly during rain

157 events (Dang et al., 2015b).

158 All solid fractions were frozen (-18°C) in HDPE bottles, freeze-dried, 2-mm sieved and then

159 kept at -18°C until further treatment.

160 **2.2. Sediment analysis**

161 Total Mg, P and Iodine concentrations were determined by X-Ray Fluorescence (Philips PW

162 2400) equipped with a Rh-tube (detection limit around 0.5%). Particulate organic carbon and

163 total N were analyzed using either a TOC-V_{CSH} analyzer (Shimadzu) or an NCS Flash 2000

164 analyzer (Thermo Scientific). Analytical details and part of the data have been previously

165   published (Dang et al., 2014a, 2014b; Tessier et al., 2011). Hereafter, C or OC are used for

166   particulate organic carbon.

167   For C and N stable isotope measurements, sediments were exposed to concentrated HCl vapor

168   for four days to remove the carbonate matrix. Samples of a few mg were then weighted in tin

169   capsules and analyzed at the Water Quality Centre (WQC), Trent University, Canada on a

170   Micromass (Isoprime) Continuous Flow Isotope Ratio Mass Spectrometer (CF-IRMS),

171   equipped with a Eurovector Elemental Analyzer (EA) for sample introduction. Several blanks

172   and certified reference materials (i.e., USGS 40 Glutamic Acid Standard, DG(A1) Glutamic

173   Acid Standard, Casein and High Organic Sediment standard (OAS)) bracketed the samples. A

174   comparison of the analyzed and certified values is shown in Figure S1. The δ^{13}C and δ^{15}N

175   isotopic ratios are expressed in the usual δ-notation (part per mil, ‰), relative to Vienna

176   PeeDee Belemnite for C and atmospheric N_2 for N.

177   **2.3. Stable isotope mixing model: IsoSource**

178   IsoSource version 1.3.1 (Phillips et al., 2005; Phillips and Gregg, 2003) was used for source

179   separation, similar to Das et al. (2008). Typically, C and N isotopic composition of several

180   sources are implemented as inputs of different endmembers. For a sediment sample

181   (considered as Mixture), the program determines a range of feasible solutions of source

182   contribution as there are too many combinations to allow a single solution (when the number

183   of sources is higher than the number of used isotope signatures). For n sources S_i, the

184   observed isotopic signature of the Mixture is the sum of products of individual contribution

185   (f_i) and corresponding signature of the source S_i ($\delta^{13}C_i$):

$$\delta^{13}C_{obs} = \sum_1^n f_i \times \delta^{13}C_i$$

186   With $\sum_1^n f_i = 1$. Same assumption is made for δ^{15}N.

8

187 Examination of relative contributions of each source was performed with small increments

188 (1%) and tolerance (0.1). Individual implemented sources in this study will be detailed in

189 following sections.

190

191 **3. RESULTS AND DISCUSSION**

192 **3.1. C, N and P distribution in sediments**

193 The OC and P profiles at station 3B, 12 and 15 were already shown and discussed previously

194 (Dang et al., 2014b). Averaged concentration in C, N of particles from the two rivers, surface

195 sediments, and sediment cores at eight stations are summarized in Table 1. Concentrations of

196 C and P in surface sediments of the whole Bay are shown in Figure 2. Globally, the C and N

197 profiles are stable all along the core (Dang et al., 2014b) while P profiles, except at station

198 MIS, are stable from the bottom of the core up to -15 cm then increase to the surface (Figure

199 S2). This profile has been reported in other coastal environments (Anschutz et al., 2007;

200 Krom and Berner, 1981) and attributed to either a P loss from sediments to porewater and/or

201 an upward diffusive flux of P which is scavenged in ferric oxyhydroxide precipitates at the

202 SWI (Krom and Berner, 1981; Ruttenberg, 2003). Although the C and P concentrations in

203 surface sediments at the scale of the Bay average ca. 3.9 ±1.5 % and 530 ±150 g g $^{-1}$ (Table

204 1), some hot spots in C and P can be noticed: northern parts of little Bay, the aquaculture area

205 (station 15), and the two outlets of treated sewage (Figure 2) which could suggest there is

206 non-point (land runoff) and point (aquaculture, sewage outlet) sources in the Bay. However, a

207 possibility of stronger diagenetic activities at these locations leading to stronger P

208 accumulation could not be excluded. Also, such surface mapping seems to show a dilution

209 effect of the Las River particles to the sediment in the north of the Little Bay (Fig. 2); as

210 particles transported in the Las River consisted of low C, N and P (0.9 %, 0.07 % and 410 g

9

211 g^{-1}, respectively), lower than that of the Eygoutier River (3 %, 0.21 % and 1240 g g^{-1},

212 respectively). Although the two watersheds are karstic, Eygoutier River takes it source from

213 an agricultural area, when the Dardennes dam upstream in the Las should hold back

214 significantly on particle discharge (Dufresne, 2014; Nicolau et al., 2012). These peculiarities

215 should explain the difference between the contents of C, N and P in the two rivers.

216 Also, particles from the 2 rivers have similar C/N ratios (*ca.* 14.2 g g^{-1}) and surface and

217 sediment cores presented higher values in C/N ratio (up to 44.9 g g^{-1}, Fig. 3A). Even when

218 considering a potential contribution of marine plankton (C/N ratio of 6.6, (Redfield et al.,

219 1963)), such increase in C/N ratio in sediments compared to sources (terrestrial particles

220 and/or marine planktons) could be due to the diagenetic preferential degradation of N-rich

221 compounds (Burdige, 2007; Hammond et al., 1999). In fact, a previous study has shown that

222 the C/N ratio in porewaters at station 12 was 8.6 (g g^{-1}, r^2=0.9, n = 275) (Dang et al., 2014a)

223 when the C/N ratio observed in station-12 sediments was 18.6 g g^{-1} (Figure 3A). Compared to

224 the C/N ratio of the river particles of 14.2 g g^{-1} (Figure 3A), this observation confirms the

225 diagenetic degradation of N-rich compounds leading to an N-depletion in sediments and N-

226 enrichment in porewater. Moreover, it seems that the C and N mass balance is preserved

227 between the residual C and N in sediments and the biologically released C and N in

228 porewater. This makes the C/N ratio a non-suitable index to track OM source in marine

229 sediments, except when it is correctly balanced. Similarly for the C and P relationship, the

230 C/P ratio in river particles is *ca.* 25.7 g g^{-1} and a P-depletion is observed in sediments (up to

231 116.7   g   g^{-1} excluding   station   15,   Fig.   3B).

232 **3.2. C and N isotope composition**

233 Vertical profiles of δ^{13}C and δ^{15}N in river particulate matter and in sediments at eight stations

234 are summarized in Figure S3. Despite the difference in C and N concentration in particles of

235 the two rivers, C and N isotope compositions are similar with values of $\delta^{13}C$ and $\delta^{15}N$ of -28.5

236 ‰ and 5.0 ‰, respectively (Table 1). The $\delta^{13}C$ profiles in sediment cores were uniformly

237 stable; the standard deviation being less than 10% of the average value (Figure S3 A, B, Table

238 1). The $\delta^{13}C$ average ranges from -30.1 to -15.8 ‰ with the most negative values observed at

239 stations MIS, LAS1 and LAS2, probably due to the impact of the delivered particles. In these

240 three sediment cores, $\delta^{15}N$ profiles were among the most stable while other sediments cores

241 showed a clear ^{15}N depletion profile from the top to the bottom of the core (Figure S3 C, D).

242 By gathering paired values of $\delta^{13}C$ and $\delta^{15}N$ from the literature on C and N isotope

243 composition in coastal areas (Table S1 and Figure S4), three main zones including freshwater

244 phytoplankton, estuarine-marine phytoplankton and macroalgae/seagrasses (Figure S4) cover

245 most of the $\delta^{13}C$-$\delta^{15}N$ biplot in the Toulon Bay sediments (Figure 4). However, within the C

246 and N isotope signature of macroalgae/seagrasses, several studies have shown that some

247 macroalgae were more depleted in ^{13}C than seagrasses, probably due to the physiological

248 morphology and the C uptake mechanisms (Alomar et al., 2016; Hemminga and Mateo, 1996;

249 Jennings et al., 1997; Stephenson et al., 1986). Therefore, while compared to the data in the

250 Toulon Bay, we have divided the macroalgae/seagrasses group into an additional fourth group

251 containing solely ^{13}C- and ^{15}N-depleted values reported for macroalgae (Table S1, Figure S4).

252 Consequently, four natural sources are compiled from the literature (i) S1: freshwater

253 phytoplankton, (ii) S2: estuarine-marine phytoplankton, (iii) S3: seagrasses/macroalgae and

254 (iv) S4: macroalgae. In addition, one anthropogenic source (Source A) could be implemented.

255 For that, at stations MIS, 3B, 12, 15 and 23, a significant correlation between $\delta^{13}C$ and P is

256 observed (n = 28, r^2 = 0.71, p < 0.0001) reveals that such high accumulation in P (up to 1400

257 g g $^{-1}$ at station MIS) could be an anthropogenic input in the area, together with a specific

258 signature of C. The corresponding $\delta^{13}C$ of the source A was then assumed to that of the

259   sample the most concentrated in P ($\delta^{13}C_{sourceA}$ = -26.5 ‰). The $\delta^{15}N_{sourceA}$ was assumed to be

260   10 ‰, as usually found for anthropogenic N isotope composition from urban and aquaculture

261   impacts (Savage et al., 2010; Yokoyama et al., 2006). These five sources (Figure 4) have been

262   utilized in the IsoSource program to calculate the respective contribution of each individual

263   source to the observed C and N isotope composition in Toulon Bay sediments.

264   **3.3. A quantitative multiple-endmember mixing model for C and N isotope composition**

265   Outputs of the IsoSource model are relative contributions of each of five sources previously

266   defined. The modeled C and N isotope composition is compared to that observed in sediments

267   (Figure 5). For C, the model has calculated well the isotope composition of all sediments

268   (Figure 5A). However, the model has predicted well for only 80 percent of the dataset of N

269   and there is an offset of 1.15 ‰ concerning 20 % of the samples having the largest

270   contributions of Source 4 (Figure 5B). This includes the samples the most depleted in ^{15}N.

271   The offset of 1.15 ‰ falls within the error of the source 4 ($\delta^{15}N_{Source4}$ = 1.5±1.2 ‰) and the

272   difference between the average (1.5‰) and the most depleted value recorded in our sediments

273   (Figure 4). Other studies have already reported *Caulerpa sp.*, the most important invasive

274   macroalgae in the Mediterranean Sea (Alomar et al., 2016), with such depletion in ^{15}N ($\delta^{15}N$

275   = 0.3±0.43 ‰ to 1.7±0.56%) and a similar composition in C ($\delta^{13}C$ = -23±0.51 ‰ to -

276   20.1±0.26%) to our sediments (Loneragan et al., 1997). However, without a confirmation of

277   the isotopic composition of macroalgae populations in Toulon Bay, the averaged isotope

278   composition of Source4 is not shifted assuming that the model for N isotope is still considered

279   correct (slope = 1.03, r^2 = 0.79, Figure 5B) and taking into account analytical and modeling

280   errors. Also, this model did not take into account stations LAS1 and LAS2 as their C and N

281   isotopic composition did not fall in the zone defined by the five sources. That would require

282   an additional source depleted in both ^{13}C and ^{15}N (Figure 4). Such situation has been reported

283   for a coastal wetland (δ^{15}N = 0.7±0.8 ‰ and δ^{13}C -26.8±1% (Li et al., 2016)). Nevertheless,

284   without having investigated in the signature of the Toulon Bay "urban" wetland, this firth

285   natural source is not added in the model.

286   Contributions of each of the five sources to the C and N isotope composition in six sediments

287   cores are summarized in radar plots (Figure 6). For station MIS, sources 1 and 4 are dominant

288   while at the station 3B, C and N isotope compositions are predicted to be from all five sources

289   with a slightly higher contribution from source 2. Stations 12 and 15 are similar, with a strong

290   contribution of source 3. From land to sea, the contribution of Source 4 increases from land to

291   sea to reach equal contribution with Source 3 at station 23, and dominant contribution at

292   station 52. In summary, there is a transition of the relative source contributions from the coast

293   to the open part of the Bay (i.e., from station MIS to 52). Station MIS which is the most

294   northern in little Bay is strongly influenced by the terrestrial input (Source 1). Station 3B

295   which is situated in a zone where macrophytes are devastated has equal contributions from all

296   sources with a slight dominance of marine phytoplankton signature (Source 2). Stations 12

297   and 15 are located in a shallow water-column zone and have a strong seagrass signature

298   (Source 3). In the large Bay, C and N isotope compositions seemed to be depleted in ^{15}N

299   which can result from the presence of macroalgae (Source 4). However, as concentrations in

300   C and N at these stations are lower than other stations, the influence of diagenetic alteration

301   on C and N isotope composition could be more significant than for the rest of the Bay.

302
303   As the anthropogenic contribution could be from either non-point (runoff) or point (treated

304   sewage) sources, contributions of Source 1 (terrestrial input) and Source A (Anthropogenic

305   source) were used to evaluate the anthropogenic signature of N isotope composition

306   (δ^{15}N$_{anthr.}$):

$$\delta^{15}N_{anthr.} = f_{source1} \times \delta^{15}N_{source1} + f_{sourceA} \times \delta^{15}N_{sourceA}$$

307 For stations where these sources are recurrent, this calculation revealed a significant

308 relationship between total P and $\delta^{15}N_{anthr.}$ rather than $\delta^{15}N_{bulk}$ (Figure 7); this P-$\delta^{15}N_{anthr.}$

309 relationship involves stations MIS, 3B and 12, demonstrating a potential co-contamination of

310 P and anthropogenic N in the northern part of the Bay. On the other hand, when comparing

311 total P to total I and Mg in sediments of the whole system (Figure 8), strong relationships are

312 observed among them, only at stations 15, 23 and 52 but not for those where P is correlated to

313 $\delta^{15}N_{anthr.}$ (i.e., MIS, 3B and 12). In fact, Iodine is released in sediment porewater as an organic

314 matter decomposition product in anoxic conditions, then converted into solid phases in oxic

315 conditions due to the affinity to iron oxyhydroxide (Gao et al., 2003; Ullman and Aller, 1980;

316 Xianhao et al., 1992). Similar diagenetic behavior is stated for P (Ruttenberg, 2003). In

317 addition, there is a negative correlation between Mg and P at stations 15, 23 and 52 (Figure

318 8B), which confirms once again that P accumulation in these stations is related to diagenetic

319 processes as Mg is accumulated by carbonate mineral precipitation where CO_2 is released

320 from organic carbon oxidation (Metzger et al., 2007). The correlation between Iodine, Mg and

321 P in sediments at station 15, 23 and 52 (Figure 8) supports the hypothesis that diagenetic

322 reactions are the major processes leading to P accumulation at these stations but not an

323 additional anthropogenic input. These approaches (as shown in Figures 7 and 8) allow us to

324 differentiate the anthropogenic and "non-anthropogenic/diagenetic" pools of P in coastal

325 sediments.

326 Eventually, applying the multiple end-member mixing model for C and N and the relationship

327 to P for the surface sediments of the whole Toulon Bay ($P_{anthr.} = 270 \times \delta^{15}N_{anthr.}$, Figure 7),

328 surface (0-5 cm) distribution of anthropogenic P was calculated (Figure 9). This revealed a

329 non-point source with strong P loading in the northern part of the little Bay and several point

14

330   sources at stations 15 (aquaculture area), 39 and 42 (treated sewage outlet). This supports not

331   only the validity of the model but also the applicability of the approach to detecting

332   anthropogenic P loading in coastal sediments. This approach seems to be more refined than

333   using total OC and/or P as shown in Figure 2.

334   In addition, the non-anthropogenic P is calculated as the difference between total P and $P_{anthr.}$

335   in six sediments cores (Figure 10). The applied model allowed us to assess the background of

336   P in the Bay and revealed P accumulation only by diagenetic reactions just below the SWI.

337   Indeed, from various profiles of total P in several sediments cores within the Bay (range of

338   300-2000 μg g^{-1}, Figure S2), the non-anthropogenic P profiles for six stations were identical

339   (Figure 10A) with a typical stable background P concentration of 350±60 (2sd) μg g^{-1} and an

340   diagenetic accumulation leading up to 60 % of the P background concentration at the top

341   sediment layer (Figure 10B).

342

343   **4. CONCLUSIONS**

344   C and N isotope ratios have been proven to be useful proxies to (i) decode biogeochemical

345   processes involving the organic matter, (ii) to study the food web and (iii) to assess ecological

346   impacts in a changing world. However, relatively few studies exist that have developed

347   quantitative mixing models for C and N isotopes with multiple sources taken into account.

348   This study has shown:

349   - The applicability of such quantitative multiple end-member mixing models for C and N

350   isotopes to track organic matter and nutrient sources in coastal environments.

351   - The possibility to differentiate anthropogenic N and P from diagenetic accumulation ("non-

352   anthropogenic").

353   - An estimate of point and non-point sources of P in the coastal area of Toulon Bay (runoff

354   and aquaculture-treated sewage, respectively).

355   - An evaluation of the sedimentary P background profile for the whole Bay of Toulon.

367

368   **REFERENCES**

369   Alomar, C., Deudero, S., Andaloro, F., Castriota, L., Consoli, P., Falautano, M., Sinopoli, M.,

370   2016. Caulerpa cylindracea Sonder invasion modifies trophic niche in infralittoral rocky

371   benthic   community.   Mar.   Environ.   Res.   120,   86–92.

372   doi:10.1016/j.marenvres.2016.07.010

373   Anschutz, P., Chaillou, G., Lecroart, P., 2007. Phosphorus diagenesis in sediment of the Thau

374   Lagoon. Estuar. Coast. Shelf Sci. 72, 447–456. doi:10.1016/j.ecss.2006.11.012

375   Belicka, L.L., Burkholder, D., Fourqurean, J.W., Heithaus, M.R., MacKo, S.A., Jaff́, R., 2012.

376   Stable isotope and fatty acid biomarkers of seagrass, epiphytic, and algal organic matter

377   to consumers in a pristine seagrass ecosystem. Mar. Freshw. Res. 63, 1085–1097.

378   doi:10.1071/MF12027

379   Bernard, G., Denis, J., Deneux, F., Belsher, T., Sauzade, D., Boudouresque, C.F., Charbonnel,

380   E., Emery, E., Herve, G., Bonhomme, P., 2001. Etude et cartographie des biocénoses de

381   la rade de Toulon, in: Contrat D'étude Pour Le Syndicat Intercommunal de l'Aire

382   Toulonaise, Ifremer et GISPosidonie. Ifremer Publ, La Seyne, p. 150.

383   Bohlin, H.S., Mörth, C.M., Holm, N.G., 2006. Point source influences on the carbon and

384   nitrogen geochemistry of sediments in the Stockholm inner archipelago, Sweden. Sci.

385   Total Environ. 366, 337–349. doi:10.1016/j.scitotenv.2005.07.016

386   Bouillon, S., Connolly, R.M., Gillikin, D.P., 2012. Use of Stable Isotopes to Understand Food

387   Webs and Ecosystem Functioning in Estuaries, Treatise on Estuarine and Coastal

388   Science. Elsevier Inc. doi:10.1016/B978-0-12-374711-2.00711-7

389   Burdige, D.J., 2007. Preservation of organic matter in marine sediments: controls,

390   mechanisms, and an imbalance in sediment organic carbon budgets? Chem. Rev. 107,

391   467–85. doi:10.1021/cr050347q

392   Choi, W.J., Lee, S.M., Ro, H.M., 2003. Evaluation of contamination sources of groundwater

393   NO 3− using nitrogen isotope data: A review. Geosci. J. 7, 81–87.

394   Church, T.M., Sommerfield, C.K., Velinsky, D.J., Point, D., Benoit, C., Amouroux, D., Plaa,

395   D., Donard, O.F.X., 2006. Marsh sediments as records of sedimentation, eutrophication

396   and metal pollution in the urban Delaware Estuary. Mar. Chem. 102, 72–95.

397   doi:10.1016/j.marchem.2005.10.026

398   Cloern, J., Canuel, E., Harris, D., 2002. Stable carbon and nitrogen isotope composition of

399   aquatic and terrestrial plants of the San Francisco Bay estuarine system. Limnol.

400   Oceanogr. 47, 713–729.

401   Cossa, D., Garnier, C., Buscail, R., Elbaz-Poulichet, F., Mikac, N., Patel-Sorrentino, N.,

402   Tessier, E., Rigaud, S., Lenoble, V., Gobeil, C., 2014. A Michaelis–Menten type

403   equation for describing methylmercury dependence on inorganic mercury in aquatic

404   sediments. Biogeochemistry 119, 35–43. doi:10.1007/s10533-013-9924-3

405   Cuntz, M., 2011. Carbon cycle: A dent in carbon's gold standard. Nature 477, 547–548.

406   doi:10.1038/477547a

407   Dang, D.H., Lenoble, V., Durrieu, G., Mullot, J.-U., Mounier, S., Garnier, C., 2014a.

408   Sedimentary dynamics of coastal organic matter: An assessment of the porewater
409   size/reactivity model by spectroscopic techniques. Estuar. Coast. Shelf Sci. 151, 100–
410   111. doi:10.1016/j.ecss.2014.10.002

411   Dang, D.H., Lenoble, V., Durrieu, G., Omanović, D., Mullot, J.-U., Mounier, S., Garnier, C.,
412   2015a. Seasonal variations of coastal sedimentary trace metals cycling: Insight on the
413   effect of manganese and iron (oxy)hydroxides, sulphide and organic matter. Mar. Pollut.
414   Bull. 92, 113–124. doi:10.1016/j.marpolbul.2014.12.048

415   Dang, D.H., Schaefer, J., Brach-Papa, C., Lenoble, V., Durrieu, G., Dutruch, L., Chiffoleau,
416   J.-F., Gonzalez, J.-L., Blanc, G., Mullot, J.U., Mounier, S., Garnier, C., 2015b.
417   Evidencing the impact of coastal contaminated sediments on mussels through Pb stable
418   isotopes composition. Environ. Sci. Technol. 49, 11438–11448.
419   doi:10.1021/acs.est.5b01893

420   Dang, D.H., Tessier, E., Lenoble, V., Durrieu, G., Omanović, D., Mullot, J.-U., Pfeifer, H.-R.,
421   Mounier, S., Garnier, C., 2014b. Key parameters controlling arsenic dynamics in coastal
422   sediments: an analytical and modeling approach. Mar. Chem. 161, 34–46.

423   Das, B., Nordin, R., Mazumder, A., 2008. An alternative approach to reconstructing organic
424   matter accumulation with contrasting watershed disturbance histories from lake
425   sediments. Environ. Pollut. 155, 117–124. doi:10.1016/j.envpol.2007.10.031

426   Dean, W.E., 2006. Characterization of Organic Matter in Lake Sediments from Minnesota and
427   Yellowstone National Park, U.S. Geological Survey Open-File Report 2006-1053.

428   Di Leonardo, R., Cundy, A.B., Bellanca, A., Mazzola, A., Vizzini, S., 2012. Biogeochemical
429   evaluation of historical sediment contamination in the Gulf of Palermo (NW Sicily):
430   Analysis of pseudo-trace elements and stable isotope signals. J. Mar. Syst. 94, 185–196.
431   doi:10.1016/j.jmarsys.2011.11.022

432   Dufresne, C., 2014. Compréhension et analyse des processus hydrosédimentaires dans la baie
433   de Toulon. Apport à la modélisation de la dispersion des radionucléides. Université de
434   Toulon.

435   Engel, M., Macko, S.A., 2013. Organic Geochemistry: Principles and Applications. Springer
436   Science & Business Media.

437   Erhardt, E.B., Wolf, B.O., Ben-David, M., Bedrick, E.J., 2014. Stable Isotope Sourcing Using
438   Sampling. Open J. Ecol. 4, 289–298. doi:10.4236/oje.2014.46027

439   Gao, A.G., Liu, Y.G., Zhang, D.J., Sun, H.Q., 2003. Latitudinal distribution of iodine in
440   sediments in the Chukchi Sea and the Bering Sea. Sci. China Ser. D-Earth Sci. 46, 592–
441   602. doi:10.1360/03yd9052

442   Hammond, D.E., Giordani, P., Berelson, W.M., Poletti, R., 1999. Diagenesis of carbon and
443   nutrients and benthic exchange in sediments of the Northern Adriatic Sea. Mar. Chem.
444   53–79.

445   Harmelin-Vivien, M., Loizeau, V., Mellon, C., Beker, B., Arlhac, D., Bodiguel, X., Ferraton,
446   F., Hermand, R., Philippon, X., Salen-Picard, C., 2008. Comparison of C and N stable
447   isotope ratios between surface particulate organic matter and microphytoplankton in the
448   Gulf of Lions (NW Mediterranean). Cont. Shelf Res. 28, 1911–1919.
449   doi:10.1016/j.csr.2008.03.002

450   Hemminga, M.A., Mateo, M.A., 1996. Stable carbon isotopes in seagrasses: Variability in
451   ratios and use in ecological studies. Mar. Ecol. Prog. Ser. 140, 285–298.
452   doi:10.3354/meps140285

453   Hobbie, J.E., 2000. Estuarine Science: A Synthetic Approach to Research and Practice.
454   Washington, DC.

455   Jamet, J.L., Jean, N., Bogé, G., Richard, S., Jamet, D., 2005. Plankton succession and
456   assemblage structure in two neighbouring littoral ecosystems in the north-west
457   Mediterranean Sea. Mar. Freshw. Res. 56, 69–83. doi:10.1071/MF04102

458   Jean, N., Dumont, E., Durrieu, G., Balliau, T., Jamet, J.-L., Personnic, S., Garnier, C., 2012.
459   Protein expression from zooplankton communities in a metal contaminated NW
460   mediterranean coastal ecosystem. Mar. Environ. Res. 80, 12–26.
461   doi:10.1016/j.marenvres.2012.06.004

462   Jennings, S., Reñones, O., Morales-Nin, B., Polunin, N.V.C., Moranta, J., Coll, J., 1997.
463   Spatial variation in the 15N and 13C stable isotope composition of plants, invertebrates
464   and fishes on Mediterranean reefs: Implications for the study of trophic pathways. Mar.
465   Ecol. Prog. Ser. 146, 109–116. doi:10.3354/meps146109

466   Kendall, C., Silva, S.R., Kelly, V.J., 2001. Carbon and nitrogen isotopic compositions of
467   particulate organic matter in four large river systems across the United States. Hydrol.
468   Process. 15, 1301–1346. doi:10.1002/hyp.216

469   Kimbrough, K.L., Johnson, W.E., Lauenstein, G.G., Chrstensen, J.D., Apeti, D.A., 2008. An
470   assessment of two decades of contaminant monitoring in the nation's coastal zone. Silver
471   Spring, MD. NOAA Technical Memorandum NOS NCCOS 74. Silver Spring, MD.

472   Kohzu, A., Imai, A., Ohkouchi, N., Fukushima, T., Kamiya, K., Komatsu, K., Tomioka, N.,
473   Kawasaki, N., Miura, S., Satou, T., 2011. Direct evidence for the alteration of 13C
474   natural abundances during early diagenesis in Lake Kasumigaura, Japan. Geochemistry,
475   Geophys. Geosystems 12, 1–14. doi:10.1029/2011GC003532

476   Krom, M.D., Berner, R.A., 1981. The diagenesis of phosphorus in a nearshore marine
477   sediment. Geochim. Cosmochim. Acta 45, 207–216. doi:10.1016/0016-7037(81)90164-2

478   Lehmann, M., Bernasconi, S., Barbieri, A., McKenzie, J., 2002. Preservation of organic
479   matter and alteration of its carbon and nitrogen isotope composition during simulated
480   and in situ early sedimentary diagenesis. Geochim. Cosmochim. Acta 66, 3573–3584.
481   doi:10.1016/S0016-7037(02)00968-7

482   Li, Y., Zhang, H., Tu, C., Fu, C., Xue, Y., Luo, Y., 2016. Sources and fate of organic carbon
483   and nitrogen from land to ocean: Identified by coupling stable isotopes with C/N ratio.
484   Estuar. Coast. Shelf Sci. 181, 114–122. doi:10.1016/j.ecss.2016.08.024

485   Loneragan, N.R., Bunn, S.E., Kellaway, D.M., 1997. Are mangroves and seagrasses sources
486   of organic carbon for penaeid prawns in a tropical Australian estuary? A multiple stable-
487   isotope study. Mar. Biol. 130, 289–300. doi:10.1007/s002270050248

488   Metzger, E., Simonucci, C., Viollier, E., Sarazin, G., Prévot, F., Jézéquel, D., 2007. Benthic
489   response to shellfish farming in Thau lagoon: Pore water signature. Estuar. Coast. Shelf
490   Sci. 72, 406–419. doi:10.1016/j.ecss.2006.11.011

491   Meyers, P.A., 1997. Organic geochemical proxies of paleoceanographic, plaeolimnologic, and
492   plaeoclimatic processes. Org. Geochem. 27, 213–250.

493   Nicolau, R., Lucas, Y., Merdy, P., Raynaud, M., 2012. Base flow and stormwater net fluxes
494   of carbon and trace metals to the Mediterranean sea by an urbanized small river. Water

495   Res. 46, 6625–6637. doi:10.1016/j.watres.2012.01.031

496   Ogrinc, N., Fontolan, G., Faganeli, J., Covelli, S., 2005. Carbon and nitrogen isotope
497   compositions of organic matter in coastal marine sediments (the Gulf of Trieste, N
498   Adriatic Sea): Indicators of sources and preservation. Mar. Chem. 95, 163–181.
499   doi:10.1016/j.marchem.2004.09.003

500   Paerl, H., 2008. Nutrient and other environmental controls of harmful cyanobacterial blooms
501   along the freshwater-marine continuum. Adv. Exp. Med. Biol. 619, 217–37.
502   doi:10.1007/978-0-387-75865-7_10

503   Paerl, H.W., 2006. Assessing and managing nutrient-enhanced eutrophication in estuarine and
504   coastal waters: Interactive effects of human and climatic perturbations. Ecol. Eng. 26,
505   40–54. doi:10.1016/j.ecoleng.2005.09.006

506   Parker, P., 1964. The biogeochemistry of the stable isotopes of carbon in a marine bay.
507   Geochim. Cosmochim. Acta 28, 1155–1164. doi:10.1016/0016-7037(64)90067-5

508   Phillips, D.L., Gregg, J.W., 2003. Source partitioning using stable isotopes: Coping with too
509   many sources. Oecologia 136, 261–269. doi:10.1007/s00442-003-1218-3

510   Phillips, D.L., Inger, R., Bearhop, S., Jackson, A.L., Moore, J.W., Parnell, A.C., Semmens,
511   B.X., Ward, E.J., 2014. Best practices for use of stable isotope mixing models in food-
512   web studies. Can. J. Zool. 835, 823–835.

513   Phillips, D.L., Newsome, S.D., Gregg, J.W., 2005. Combining sources in stable isotope
514   mixing models: Alternative methods. Oecologia 144, 520–527. doi:10.1007/s00442-004-
515   1816-8

516   Pougnet, F., Schäfer, J., Dutruch, L., Garnier, C., Tessier, E., Dang, D.H., Lanceleur, L.,
517   Mullot, J.-U., Lenoble, V., Blanc, G., 2014. Sources and historical record of tin and
518   butyl-tin species in a Mediterranean bay (Toulon Bay, France). Environ. Sci. Pollut. Res.
519   Int. 21, 6640–51. doi:10.1007/s11356-014-2576-6

520   Ramaswamy, V., Gaye, B., Shirodkar, P. V., Rao, P.S., Chivas, A.R., Wheeler, D., Thwin, S.,
521   2008. Distribution and sources of organic carbon, nitrogen and their isotopic signatures
522   in sediments from the Ayeyarwady (Irrawaddy) continental shelf, northern Andaman
523   Sea. Mar. Chem. 111, 137–150. doi:10.1016/j.marchem.2008.04.006

524   Redfield, A.C., Ketchum, B.H., Richards, F.A., 1963. The Influence of Organisms on the

525   Composition of Sea Water. Sea.

526   Ruttenberg, K.C., 2003. The Global phosphorus cycle, in: Turekian, K.K., Holland, H.D.

527   (Eds.), Treatise on Geochemistry. Elsevier Ltd, pp. 585–643.

528   Savage, C., Leavitt, P.R., Elmgren, R., 2010. Effects of land use, urbanization, and climate

529   variability on coastal eutrophication in the Baltic Sea. Limnol. Oceanogr. 55, 1033–

530   1046. doi:10.4319/lo.2010.55.3.1033

531   Stephenson, R., Tan, F., Mann, K., 1986. Use of stable carbon isotope ratios to compare plant

532   material and potential consumers in a seagrass bed and a kelp bed in Nova Scotia,

533   Canada. Mar. Ecol. Prog. Ser. 30, 1–7. doi:10.3354/meps030001

534   Teranes, J.L., Bernasconi, S.M., 2000. The record of nitrate utilization and productivity

535   limitation provided by d15N values in lake organic matter—. A study of sediment trap

536   and core sediments from Baldeggersee, Switzerland. Limnol. Oceanogr. 45, 801–813.

537   doi:10.4319/lo.2000.45.4.0801

538   Tessier, E., Garnier, C., Mullot, J.-U., Lenoble, V., Arnaud, M., Raynaud, M., Mounier, S.,

539   2011. Study of the spatial and historical distribution of sediment inorganic contamination

540   in the Toulon bay (France). Mar. Pollut. Bull. 62, 2075–2086.

541   doi:10.1016/j.marpolbul.2011.07.022

542   Ullman, W.J., Aller, R.C., 1980. Dissolved iodine flux from estuarine sediments and

543   implications for the enrichment of iodine at the sediment water interface. Geochim.

544   Cosmochim. Acta 44, 1177–1184. doi:10.1016/0016-7037(80)90071-X

545   UNEP, 2006. Marine and coastal ecosystem and human well-being: A synthesis report based

546   on the findings of the Millennium Ecosystem Assessment.

547   Vaalgamaa, S., Sonninen, E., Korhola, A., Weckström, K., 2013. Identifying recent sources of

548   organic matter enrichment and eutrophication trends at coastal sites using stable nitrogen

549   and carbon isotope ratios in sediment cores. J. Paleolimnol. 50, 191–206.

550   doi:10.1007/s10933-013-9713-y

551   Vitousek, P.M., Mooney, H. a, Lubchenco, J., Melillo, J.M., 1997. Human Domination of

552   Earth' s Ecosystems. Science (80-.). 277, 494–499. doi:10.1126/science.277.5325.494

553   Wetz, M.S., Hales, B., Wheeler, P.A., 2008. Degradation of phytoplankton-derived organic
554   matter: Implications for carbon and nitrogen biogeochemistry in coastal ecosystems.
555   Estuar. Coast. Shelf Sci. 77, 422–432. doi:10.1016/j.ecss.2007.10.002

556   Xianhao, C., Weiping, X., Haisheng, Z., 1992. Remobilization and accumulation of iodine in
557   marine sediments, Western Antartic ocean. Antarct. Res. 3, 50–59.

558   Yokoyama, H., Abo, K., Ishihi, Y., 2006. Quantifying aquaculture-derived organic matter in
559   the sediment in and around a coastal fish farm using stable carbon and nitrogen isotope
560   ratios. Aquaculture 254, 411–425. doi:10.1016/j.aquaculture.2005.10.024

561

Table 1: Concentration in OC, N, P, C/N ratio and C, N isotope composition in river particles, surface sediments and sediments core collected from Toulon Bay.

Stations	{OC} in % (n)	{N} in % (n)	C/N (g g^{-1})	δ^{13}C (‰)	δ^{15}N (‰)	{P} in g g^{-1} (n)	
Las river particles	0.9 ± 0.6 (5)	0.07 ± 0.04 (5)	14.5 ± 2	-28.5±0.8	5.0±0.9	410 ± 145 (5)	
Eygoutier river particles	3.0 ± 1.2 (5)	0.21 ± 0.09 (5)	13.7 ± 0.9			1240 ± 360 (5)	
Surface sediments	3.9 ± 1.5 (59)	0.11 ± 0.07 (9)	17.5 ± 3.5	-24.5 to -19.8	0.5 to 4.5	530 ± 150 (59)[a]	
MIS	4.9 ± 1.3 (4)	0.25 ± 0.06 (4)	19.4 ± 3.9	-25.5±1.1	4.0±0.8	850[b]	1200± 350 (20)[c]
LAS1	2.2 ± 0.6 (20)	0.12 ± 0.03 (20)	18.9 ± 1.8	-28.6±0.6	1.4 to 2.8	2500[b]	550± 90 (12)[c]
LAS2	2.5 ± 1.1 (25)	0.21 ± 0.14 (25)	14.5 ± 4.6	-26.4±1.4	3.0±0.6	350[b]	370± 60 (18)[c]
3B	5.3 ± 1.2 (23)	0.24 ± 0.04 (5)	18.6 ± 2	-21.5±0.6	4.8 to 8.9	1100[b]	870± 90 (16)[c]
12	4.9 ± 0.6 (29)	0.24 ± 0.02 (5)	18.6 ± 1	-18.6±1.7	2.6 to 5.1	860[b]	450± 40 (22)[c]
15	6.8 ± 1.1 (28)	0.24 ± 0.03 (8)	21.1 ± 2.3	-16.8±1.7	1.7 to 4.9	760[b]	320± 33 (21)[c]
23	3.5 ± 0.6 (5)	0.12 ± 0.02 (5)	28.1 ± 3.2	-17.9±0.7	1.8±0.2	500[b]	300± 40 (13)[c]
52	1.3 ± 1 (4)	0.08 ± 0.04 (4)	17.8 ± 4.4	-22.6±0.6	0.2 to 1.9	540[b]	360± 30 (14)[c]

[a] 0-5 cm; [b] 0-2cm; [c] -15 cm to sediment core bottom

TABLES

Table 1: Concentration in OC, N, P, C/N ratio and C, N isotope composition in river particles, surface sediments and sediments core collected from Toulon Bay.

FIGURES

Figure 1: Map of the study site showing main anthropogenic activities. Las and Eygoutier Rivers are discharging into little and large Bay, respectively. Two treated sewage submarine outlets discharge into large Bay. Cross symbols show the location of 54 surface sediments while circle symbols locate eight sediment cores. The numbers adjacent to cross symbols correspond to the surface sediment samples where C and N isotope compositions are analyzed.

Figure 2: Concentration in organic Carbon and total P in surface sediments (0-5 cm) of Toulon Bay.

Figure 3: Biplot of the relationship between C, N, and P in river particles and sediments of Toulon Bay. The OC/N relationship in Station-12 porewater is reported by Dang et al. (2014a).

Figure 4: Biplot of C and N isotope composition in rivers particles, surface and core sediments. The three area plots show data reported from the literature for freshwater phytoplankton (yellow), estuarine-marine phytoplankton (blue) and seagrasses/macroalgae (green). Refer to Figure S4 and Table S1 for more details. The black circles summarize the five potential sources used in the IsoSource program, while the grey circle positions the isotopic composition revealed in a wetland (Li et al., 2016).

Figure 5: Comparison of the modeled and observed C and N isotope composition by the multiple end-member mixing model. In the panel B, the symbol size is proportional to the contribution of Source4, the full line shows the regression passing through zero while the dashed line shows the regression line fitting the data.

Figure 6: Radar plots showing contributions of five sources at six sediment cores. Line-and-scatter plots show the average of the whole sediment core while line plots show the minimal and maximal values.

Figure 7: Total P vs. $\delta^{15}N$; black circles show the relationship between total P and N isotope composition in bulk sediments. Colored symbols represent individual sediment cores while

comparing total P to anthropogenic N isotope composition with the relationship of $P = 270 \times \delta^{15}N_{anthr.} + 415$.

Figure 8: Comparison of total P to Iodine and Mg in surface sediments and sediment cores. Correlations are only observed for stations 15, 23 and 52.

Figure 9: Map of anthropogenic P loading in the Toulon Bay revealing non-point source (northern Little Bay) and point sources (aquaculture: station 15 and treated sewage: stations 39 and 42).

Figure 10: Estimated non-anthropogenic (diagenetic) P profiles at six stations (A) and the averaged profile (B). The non-anthropogenic P background is represented by the vertical red line and the variation range in total P of six sediment cores is shown by the grey zone in (B). Refer to Figure S2 for individual total P profiles.

Figure 1
Click here to download high resolution image
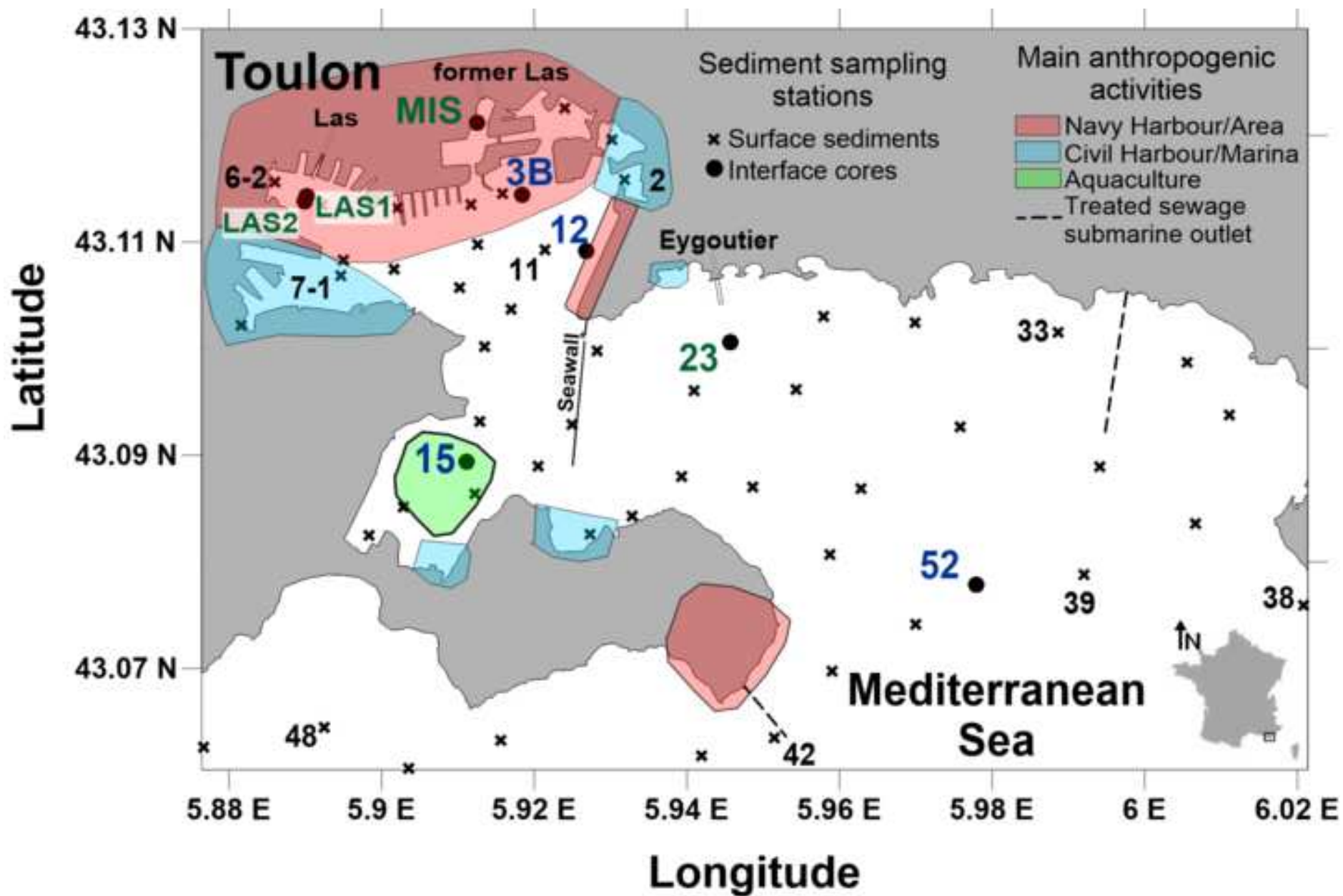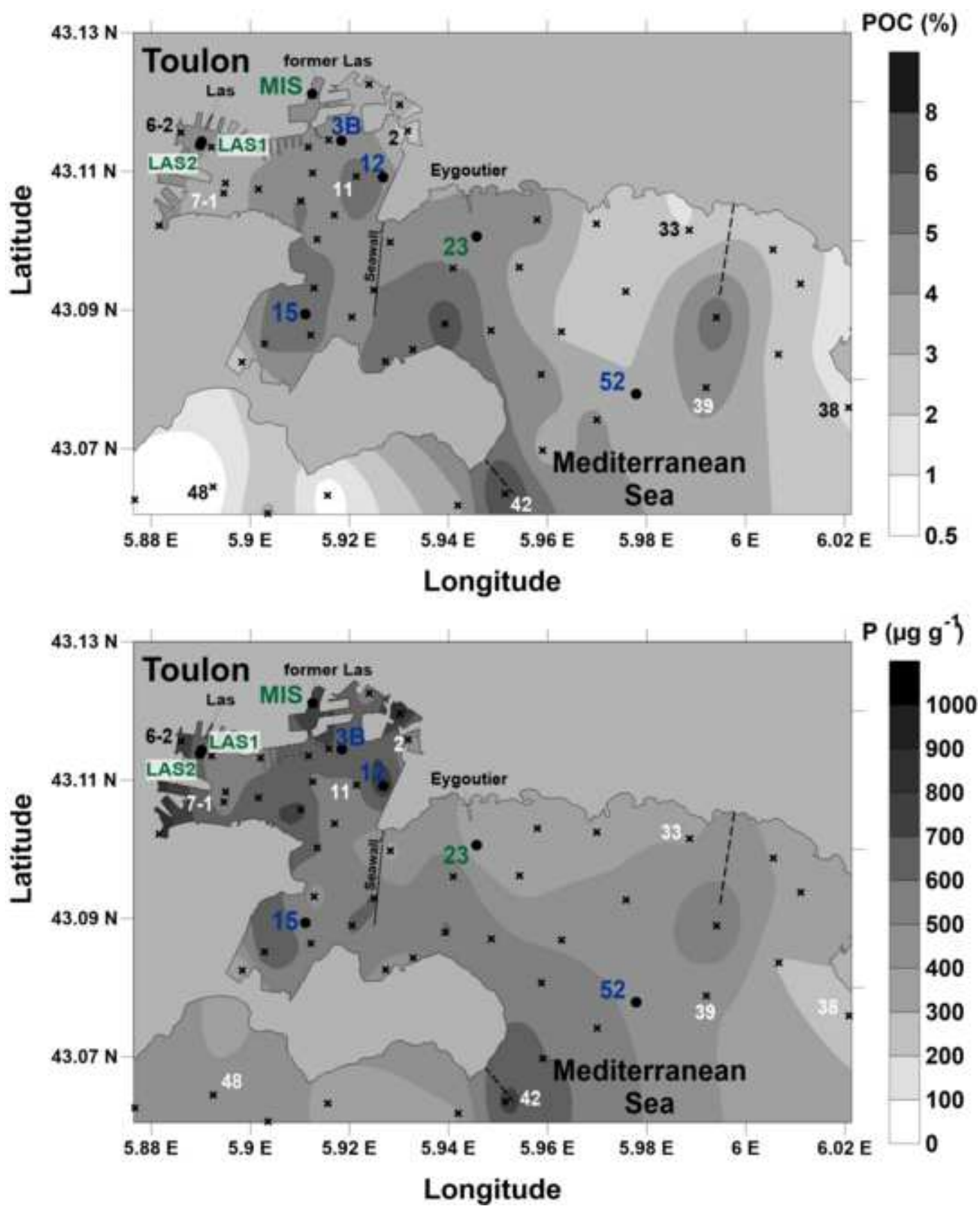
Figure 1

Figure 3
Click here to download high resolution image
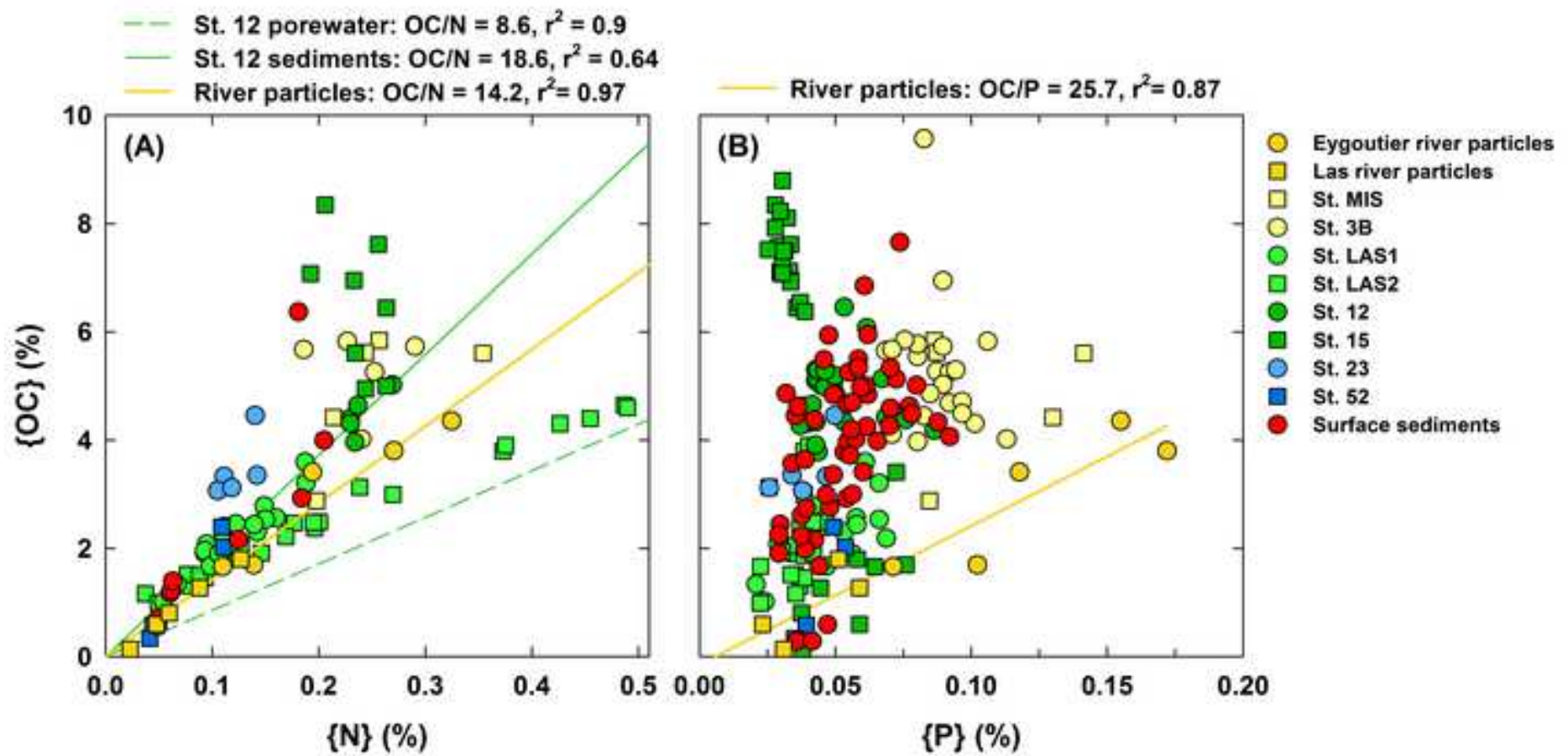
Figure 3

Figure 4
Click here to download high resolution image
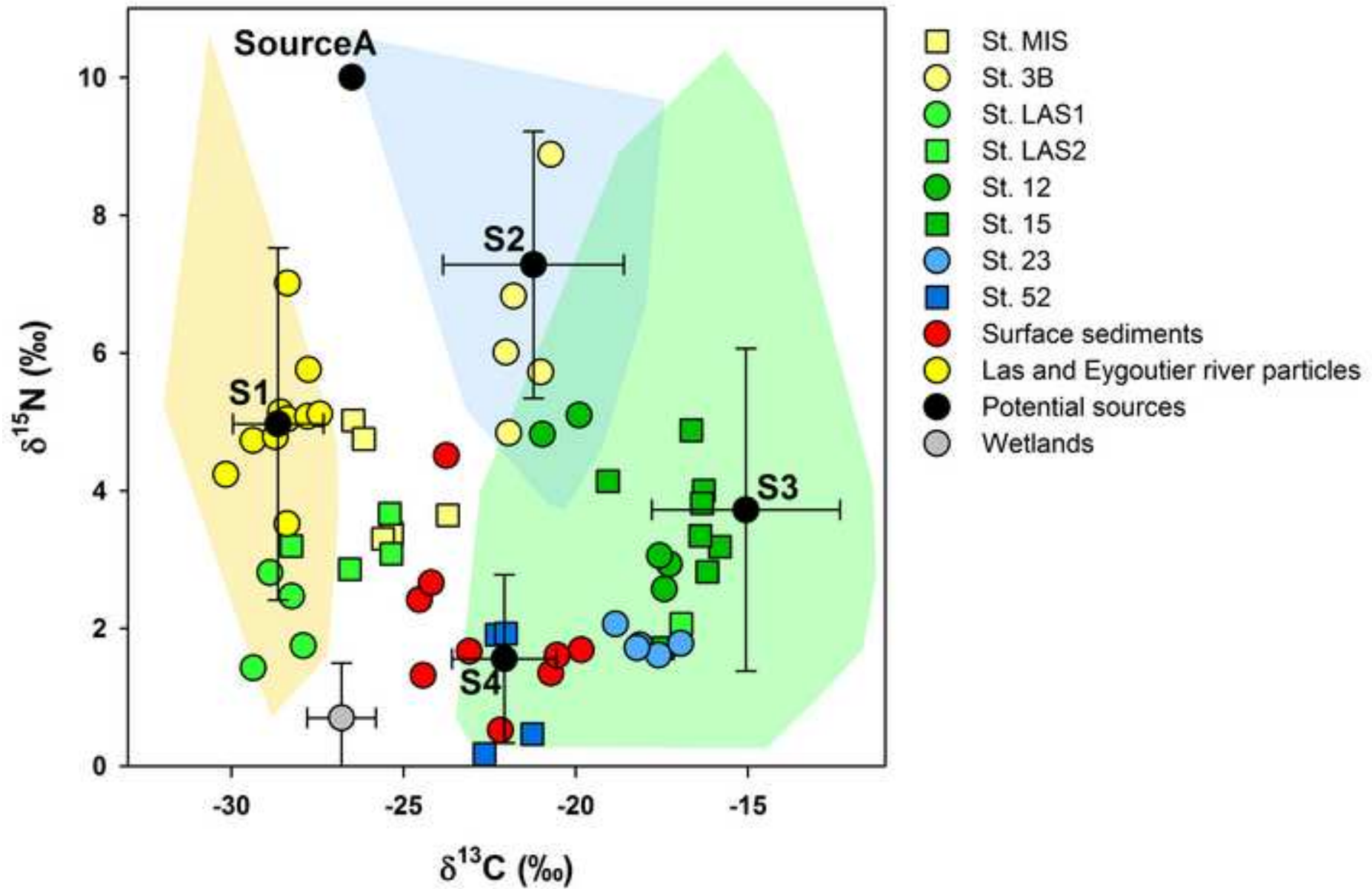
Figure 5
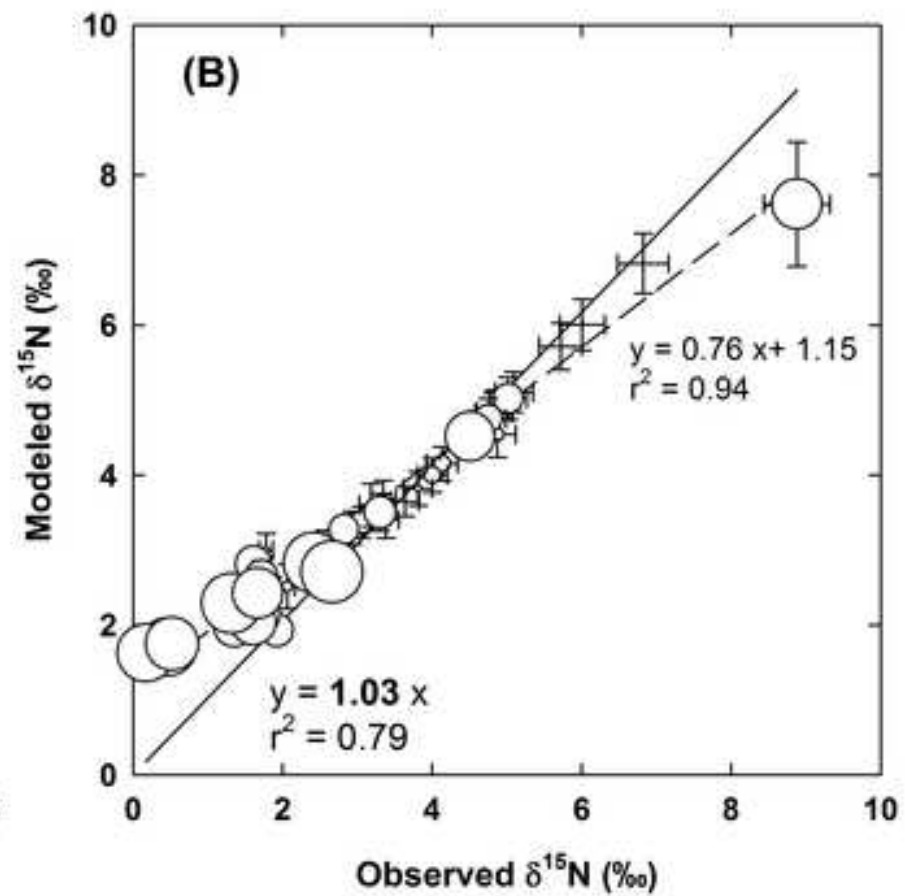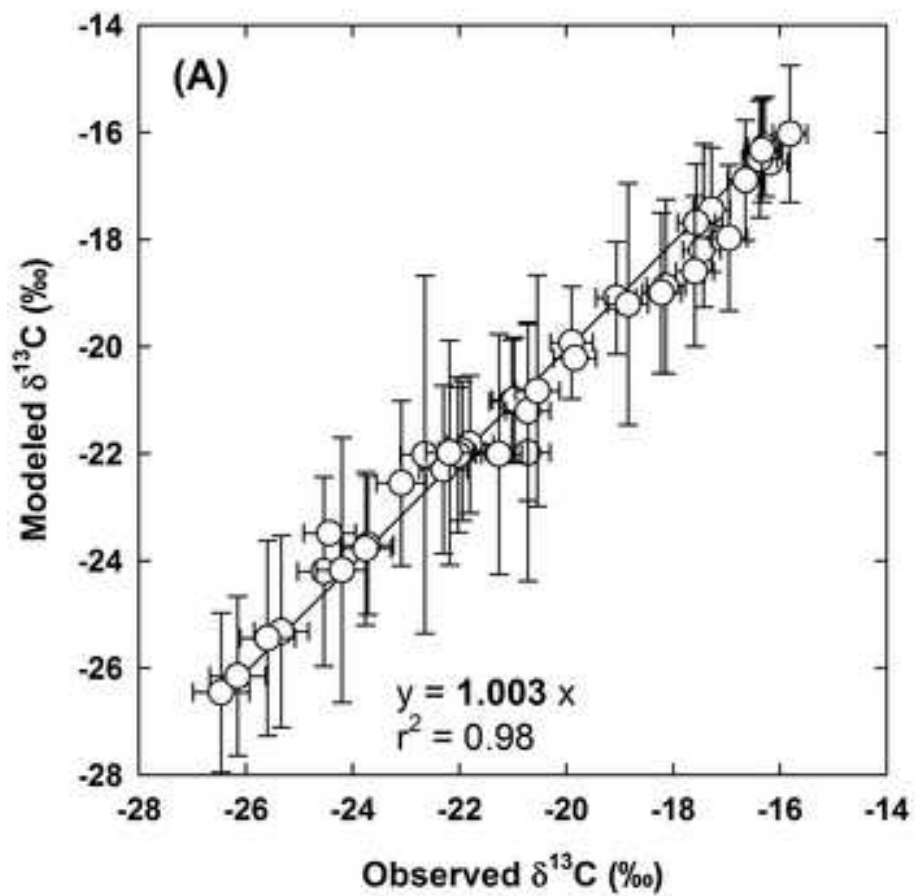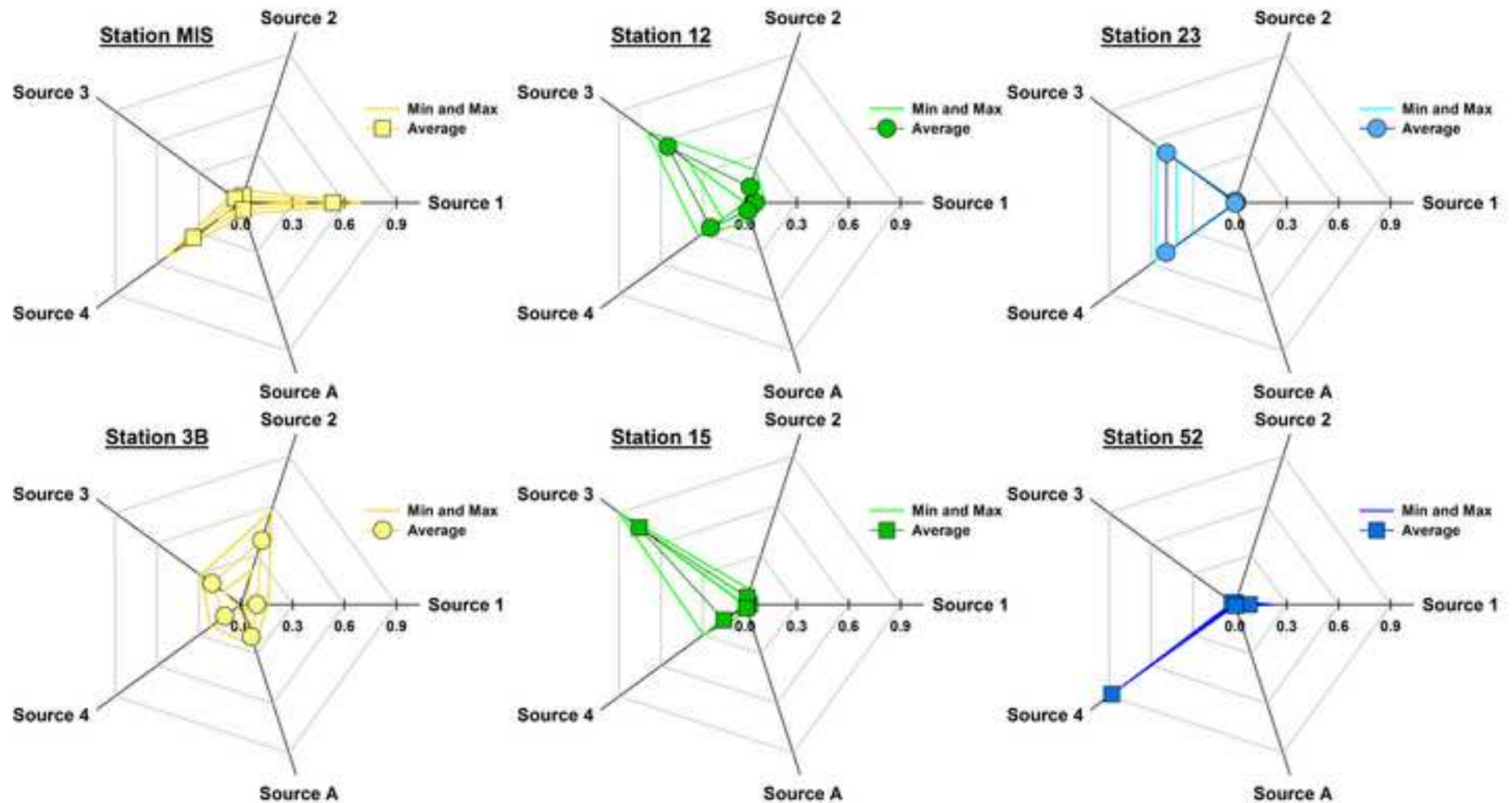
Figure 6

Figure 7

Figure 8
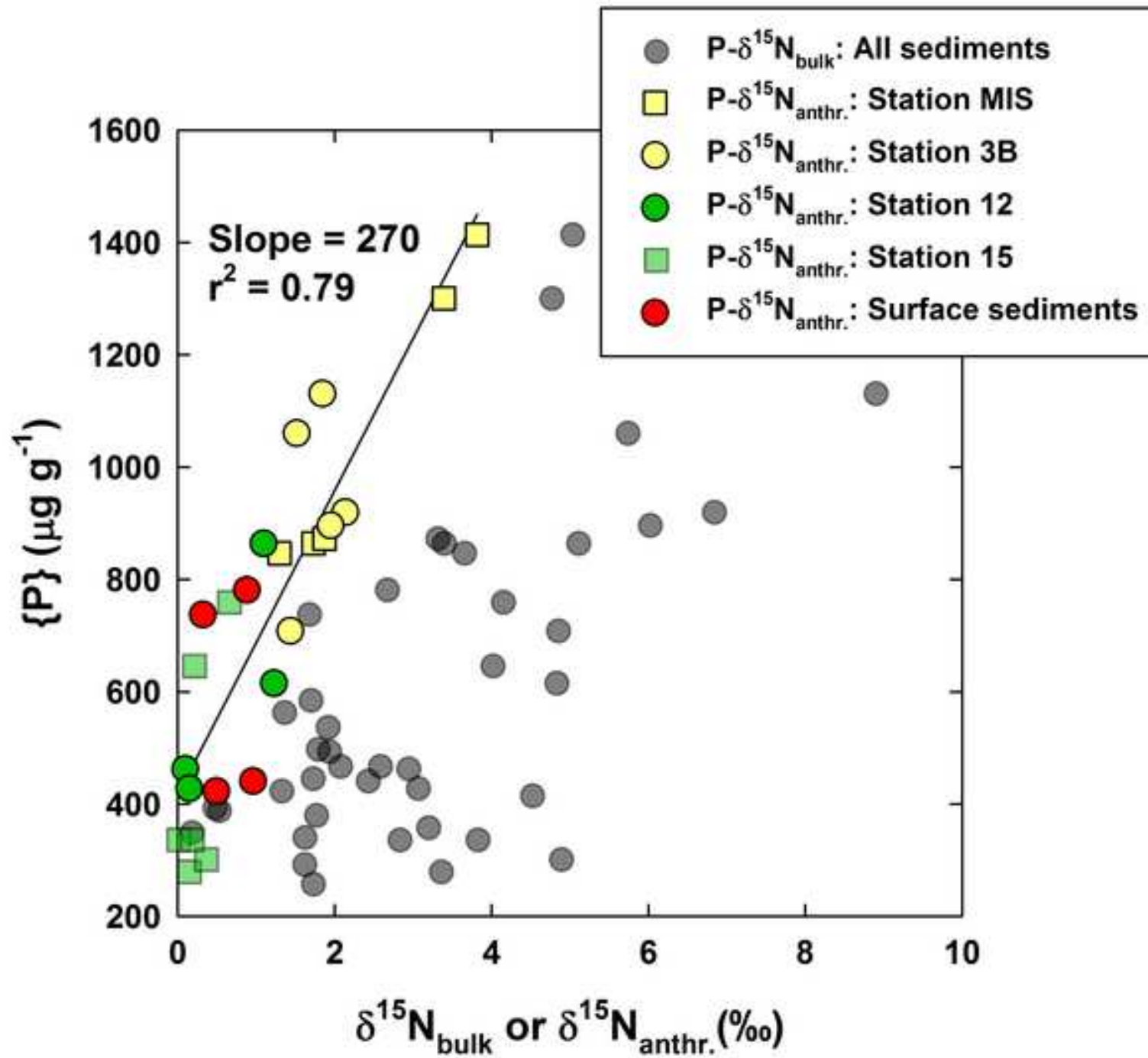**Click here to download high resolution image**
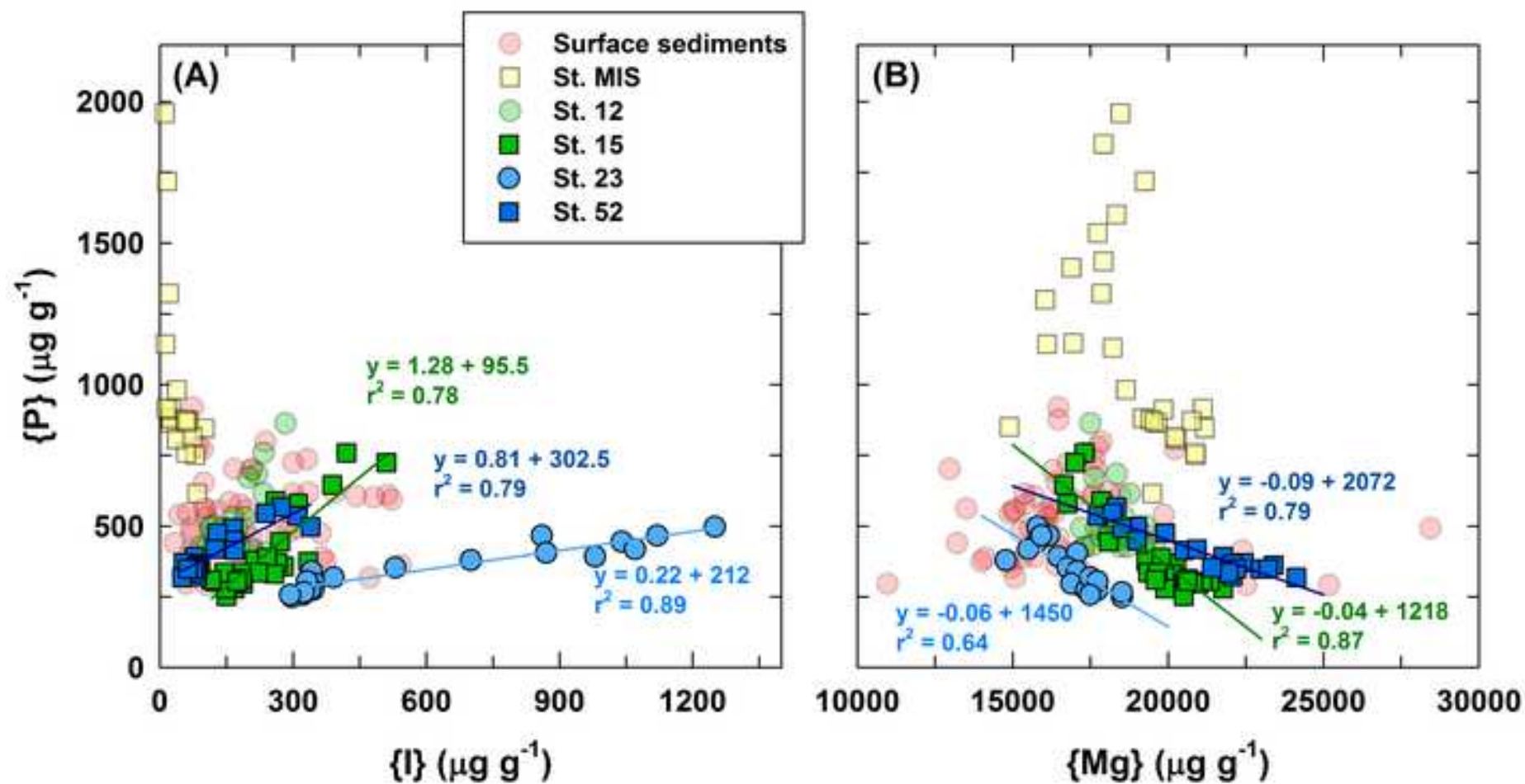
Figure 8

Figure 9
Click here to download high resolution image
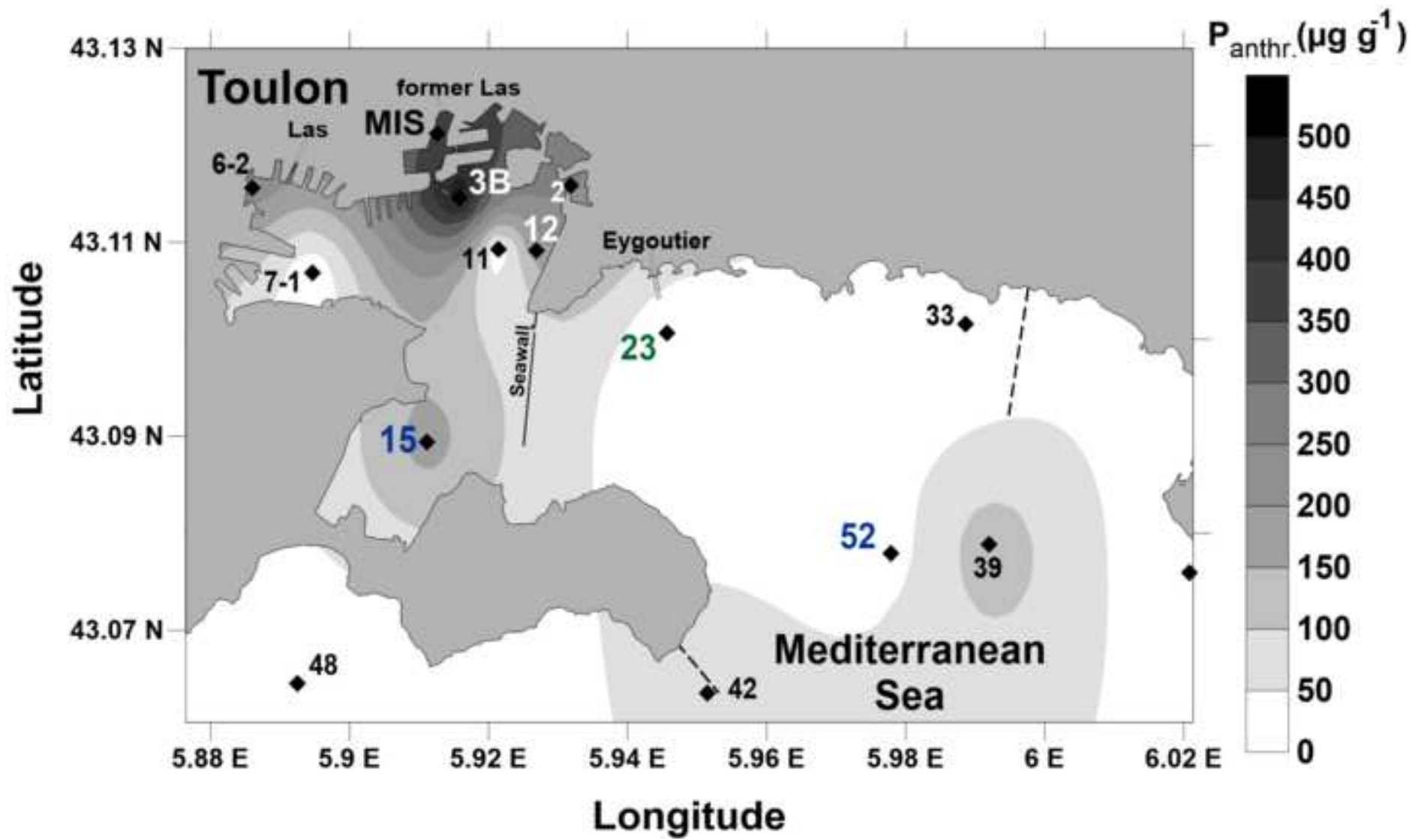
Figure 10
Click here to download high resolution image

Figure 10
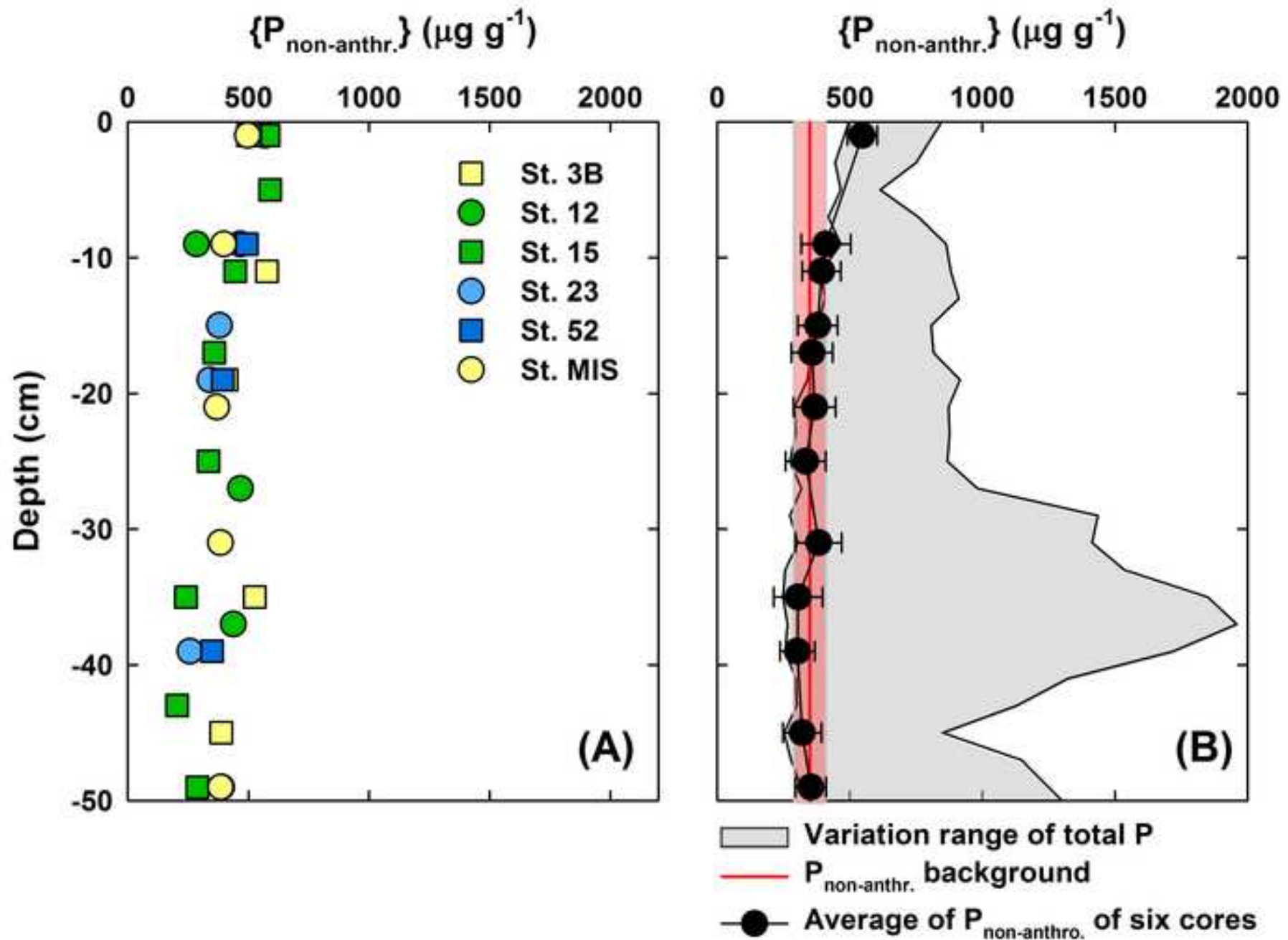
Electronic Supplementary Material (for online publication only)